arXiv:1403.7210v1 [cond-mat.mes-hall] 27 Mar 2014

Hybrid spin and valley quantum computing with singlet-triplet qubits

Niklas Rohling, Maximilian Russ, and Guido Burkard
Department of Physics, University of Konstanz, D-78457 Konstanz, Germany
(Dated: March 2014)

The valley degree of freedom in the electronic band structure of silicon, graphene, and other materials is often considered to be an obstacle for quantum computing based on electron spins in quantum dots. Here we show that control over the valley state opens new possibilities for quantum information processing. We prove that combining qubits encoded in the singlet-triplet subspace of spin and valley states allows for universal quantum computing using a universal two-qubit gate directly provided by the exchange interaction. We show how spin and valley qubits can be separated in order to allow for single-qubit rotations.

Introduction.—An alternative to single-spin qubits in quantum dots [1] is to encode each qubit in a double quantum dot (DQD) within the two-dimensional subspace spanned by the spin singlet $|S\rangle = (|01\rangle - |10\rangle)/\sqrt{2}$ and the triplet $T_0 = (|01\rangle + |10\rangle)/\sqrt{2}$ [2], with $|0\rangle = |\uparrow\rangle$, $|1\rangle = |\downarrow\rangle$. For this singlet-triplet qubit, single-qubit rotations can be realized by the exchange interaction [3, 4] and a gradient in the magnetic field [4]; two-qubit gates have been proposed based on exchange interaction [5–8] or electrostatic coupling [9–11]. An electrostatically controlled entangling gate has recently been realized experimentally [12, 13]. In this Letter we show that by extending the concept of S-T_0 qubits to electrons with spin and valley degree of freedom, the exchange interaction together with gradients in the Zeeman splittings directly provides universal quantum computing: single-qubit rotations are feasible if the spin and the valley S-T_0 qubits are stored in separated DQDs and in a dual-used DQD, i.e., containing the S-T_0 spin and valley qubits, a universal two-qubit gate can be is obtained by exchange interaction [14]. Here, we focus on operations separating and bringing together spin and valley qubits and thus allowing for the combination of single- and two-qubit operations in a quantum register. The valley degree of freedom arises from the band structure in several materials such as silicon [15], graphene [16], carbon nanotubes [17], aluminum arsenide [18], or monolayers of transition metal dichalcogenides [19, 20]. In particular, silicon-based heterostructures have recently aroused much interest as hosts for electron spin qubits [15] due to long relaxation [21] and coherence [22] times. Properties of valley states in silicon structures have been under intense investigation within the last years, both theoretically [23–38] and experimentally [39–52]. The valley degeneracy is often considered to be a problem for spin quantum computation [53, 54] and valley splitting is used to allow for pure spin exchange interaction [55]. On the other hand, theories for the manipulation of valley qubits have been developed for carbon nanotubes [56], graphene [57, 58], and silicon [59–61]. While in those approaches valley and spin qubits are considered separately, using both, spin and valley qubits, in the same quantum register is inherent in this Letter.

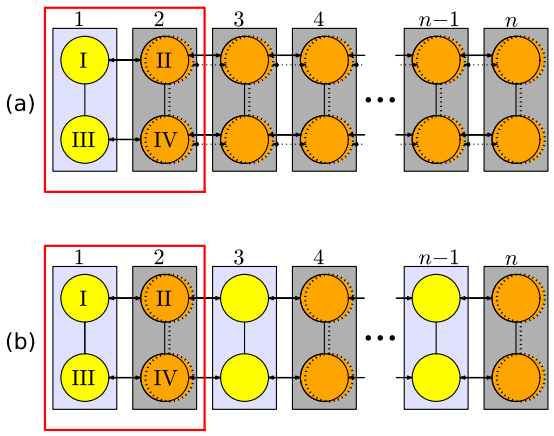

FIG. 1. Two possible quantum registers for quantum computation with spin and valley singlet-triplet qubits. The single (yellow) circles denote dots with only the spin degree of freedom (valley degeneracy lifted), whereas the double (orange) circles denote dots with both spin and valley degrees of freedom. In each DQD i with double circles, $i \geq 2$ in the register (a) and i even in (b), one spin and one valley singlet-triplet qubits can be stored. The DQDs with single circles host auxiliary spin states used to realize all quantum gates. The lines within the DQDs represent the exchange interaction (single line for spin-only dots, solid and dotted line in DQDs with spin and valley), which can realize a single qubit gate when the spin qubit is in the spin-only dots and a two-qubit gate when spin and valley qubits are in the same (orange) DQD. The arrows between dots from neighboring DQDs represent SWAP operations, allowing one to interchange the spin (solid arrow) or valley (dotted arrow) state between these dots. The register (b) has more auxiliary dots such that quantum gates can be performed with shorter sequences than in (a).

Two different types of hybrid spin-valley singlet-triplet quantum registers will be studied, as shown in Fig. 1. Both setups comprise two kinds of DQDs, one (e.g. the dots I and III) with a spin degree of freedom only (simple yellow circles), where the valley degeneracy does not exist or has been lifted, and another kind of DQD (e.g. II and IV) with both spin and two-fold valley degree of freedom marked as double orange circles. The elementary build-

ing block of the proposed quantum register consists of two DQDs, one of each kind (DQDs 1 and 2 in Fig. 1). For the encoding of quantum information we use the singlet $|S\rangle$ and triplet $|T_0\rangle$ states of spin and valley in the DQD 2 as the logical qubits. The spins in DQD 1 are spin-polarized, either $|T_+\rangle = |\uparrow\uparrow\rangle$ or $|T_-\rangle = |\downarrow\downarrow\rangle$, which is needed for the single-qubit gates. The exchange interaction between dots II and IV, described in general by a Kugel-Khomskii Hamiltonian [14, 62], already leads to a universal two-qubit gate between the spin and the valley singlet-triplet qubits in the same DQD [14]. Single-qubit gates for the logical qubits can be achieved by applying two spin-only SWAP gates, one between I and II and the other between III and IV, thereby interchanging the spin S-T_0 qubit in the DQD 2 with the polarized ancilla spins in DQD 1 without affecting the valley state. The single-qubit gates of the spin and the valley qubits can now be realized by exchange interaction and a gradient of the spin or valley Zeeman splitting [4, 60]. State preparation and measurements can be done for spatially separated spin and valley qubits. Changing the detuning within the DQD maps exactly one qubit state to a state with both electrons in one dot due to Pauli exclusion principle [63, 64]. The charge state can be detected by a quantum point contact, as realized, e.g., in Ref. [3]. State preparation can work in the opposite direction, starting from a ground state with both electrons in one dot at large detuning. Before we explain how single-qubit and two-qubit quantum gates in the quantum registers can be performed, we first propose a realization of an elementary gate in our scheme, the spin-only SWAP gate.

Model.—We consider now the system consisting of dots I and II in Fig. 1, i.e., one dot with a spin degree of freedom only and the other dot with spin and two-fold valley degree of freedom. Within our model, the physics in this DQD is described by the Hamiltonian $H = H_0 + H_T + H_V$. The influence of the detuning ε and the Coulomb repulsion energy between two electrons on the same site, U, is given by $H_0 = \varepsilon(\hat{n}_1 - \hat{n}_2)/2 + U\sum_{i=1,2}\hat{n}_i(\hat{n}_i - 1)/2$ with the number operators $\hat{n}_1 = \sum_s \hat{c}^\dagger_{1s}\hat{c}_{1s}$ and $\hat{n}_2 = \sum_{s,v}\hat{c}^\dagger_{2sv}\hat{c}_{2sv}$ where $\hat{c}^{(\dagger)}_{1s}$ is the annihilation (creation) operator of an electron with the spin state $s = \uparrow, \downarrow$ in dot 1 and $\hat{c}^{(\dagger)}_{2sv}$ is the annihilation (creation) operator of an electron with spin $s = \uparrow, \downarrow$ and valley state $v = \pm$ in dot 2. The hopping is described by $H_T = \sum_{s,v} t_v \hat{c}^\dagger_{1s}\hat{c}_{2sv} + h.c.$ and the valley splitting by $H_V = h\sum_s(\hat{c}^\dagger_{2s+}\hat{c}_{2s+} - \hat{c}^\dagger_{2s-}\hat{c}_{2s-}) \equiv h\sigma_z$, where σ_z is the corresponding Pauli matrix acting on the valley space. The sums are taken over $s = \uparrow, \downarrow$ for the spin states in the left or right dots and over the valley eigenstates $v = \pm$ in the right dot. The valley-dependent hopping elements $t_\pm$ can be expressed by [59] $t_\pm = t(1 \pm e^{i\varphi})/2$ with the real parameters t and φ. For two electrons in the dots I and II, there are 15 possible states, one with charge distribution (2,0), six with the charge distribution (0,2), and eight with the charge distribution (1,1) between dots I and II. In the limit $t \ll |h + (U \pm \varepsilon)|, |h - (U \pm \varepsilon)|$ a Schrieffer-Wolff transformation can be performed analogously to the spin-only case [65] yielding the effective Hamiltonian [66]

$$H_{\text{eff}} = [(A\cos\varphi + B)\mathbb{1} + (A + B\cos\varphi)\sigma_z + B\sin\varphi\,\sigma_y]\,P_S + \tilde{h}\sigma_z + C\,[(1 - \cos\varphi)\mathbb{1} - \sin\varphi\,\sigma_y]\,. \quad (1)$$

Here, P_S is the projector on the spin singlet $|S\rangle = (|\uparrow\downarrow\rangle - |\downarrow\uparrow\rangle)/\sqrt{2}$. The other symbols are defined as follows, $A = 4t^2Uh\varepsilon/[(h - U - \varepsilon)(h + U - \varepsilon)(h - U + \varepsilon)(h + U + \varepsilon)]$, $B = A(h^2 + \varepsilon^2 - U^2)/2h\varepsilon$, $\tilde{h} = h\{1 + t^2(1 - \cos\varphi)/[2(h - U + \varepsilon)(h + U - \varepsilon)]\}$, and $C = t^2(U - \varepsilon)/[2(h - U + \varepsilon)(h + U - \varepsilon)]$. Note that H and H_{eff} are block diagonal in a basis of singlet and triplet states for the spins, similar to the situation in Ref. [59]. Our aim is to use the term proportional to P_S in order to perform the desired spin-only SWAP gate which interchanges the spin information of dot I and II independent of the valley state. We will show that this is possible although the term in H_{eff} also acts on the valley state.

Spin-only SWAP gate.—For the valley-degenerate case $h = 0$, Eq. (1) simplifies to the mere exchange Hamiltonian

$$H^0_{\text{eff}} = -JP_SP_k - \tilde{J}P_{k^\perp}, \quad (2)$$

where $J = 4t^2U/(U^2 - \varepsilon^2)$ and $\tilde{J} = t^2/(U - \varepsilon)$. The first term is proportional to P_S and to the projector P_k on the valley state $|k\rangle = [(1 + e^{-i\varphi})|+\rangle + (1 - e^{-i\varphi})|-\rangle]/2$, which is the valley state of an electron after hopping from dot I to dot II. The second term is spin-independent and proportional to the projector $P_{k^\perp}$ on the valley state $|k^\perp\rangle = [(1 - e^{-i\varphi})|+\rangle + (1 + e^{-i\varphi})|-\rangle]/2$ orthogonal to $|k\rangle$. Both contributions originate from the Pauli principle: virtual hopping between dot I and dot II is only possible if the (0,2) or (2,0) state included in this hopping is antisymmetric. Virtual hopping from (1,1) to (0,2) and back is proportional to $t^2/(U - \varepsilon)$ and dominates for $\varepsilon \approx U$; if the valley state in the right dot is $|k^\perp\rangle$, this channel is open, independent of the spin states, as the valley state $|k\rangle$ used within the virtual hopping is empty. If the valley state is $|k\rangle$, the spins have to be in a singlet state to allow for an antisymmetric (0,2) state. Virtual hopping from (1,1) to (2,0) and back requires a valley state $|k\rangle$ in the right dot as $|k^\perp\rangle$ has no overlap with the state in the left dot. It further requires the spins to be in a singlet state to obey Fermi-Dirac statistics.

For $|U + \varepsilon| \ll U$, $\tilde{J}$ can be neglected and the time evolution $U_0(\phi) = \exp[-i\int_0^\tau d\tau' H^0_{\text{eff}}(\tau')/\hbar]$ with $\phi = \int_0^\tau d\tau' J(\tau')/\hbar$ can be computed easily, $U_0(\phi) = \mathbb{1} + (e^{i\phi} - 1)P_SP_k$. If the conditions $\tilde{J} \approx 0$, $\varphi = \pi/2$, and control ability of the valley splitting h are fulfilled, we obtain a spin-only SWAP gate with the sequence SWAP $\equiv \mathbb{1} - 2P_S = \sigma_z U_0(\pi)\sigma_z U_0(\pi)$. Here, h is turned off or at least made negligibly small during the exchange

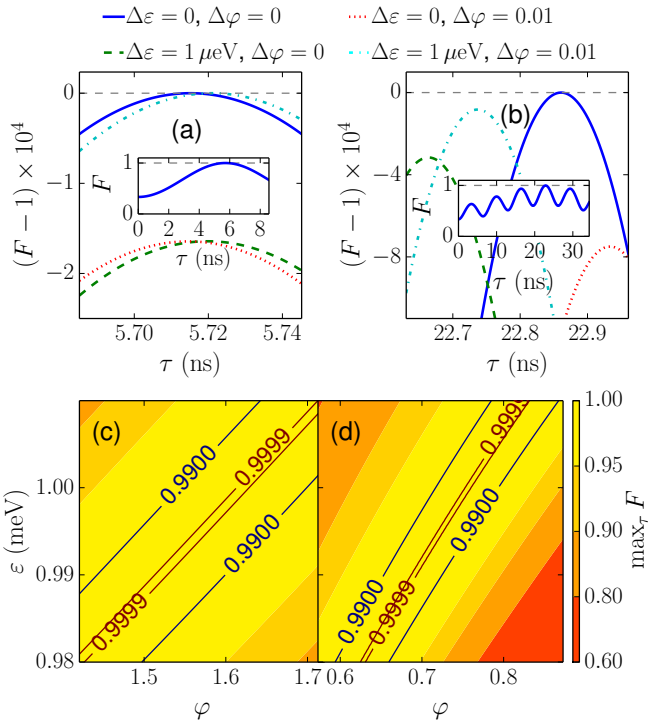

FIG. 2. Fidelity F of the time evolution operator $U_{\rm eff}(\tau)$ describing the exchange interaction between a spin-only quantum dot and a dot with spin and valley degree of freedom with respect to spin SWAP gate according to Eq. (3). The parameters are chosen to be $U = 1$ meV, $h = 0.1$ meV, $t = 6$ μeV. (a,b) F maximized over the gate time τ (scale bar). The detuning is chosen to be $\varepsilon = \sqrt{U^2 - h^2} + \Delta\varepsilon \approx 0.995$ meV$+\Delta\varepsilon$ and the phase in the hopping matrix elements, $\varphi = \arccos 0 + \Delta\varphi = \frac{\pi}{2} + \Delta\varphi$ for (a) and $\varphi = \arccos \frac{3}{4} + \Delta\varphi$ for (b). (c,d) Contour plots of maximal fidelity in dependance of ε and φ. The maximum over τ is taken numerically by searching around the first (c) or fourth (d) local maximum, respectively. We know that at $\Delta\varphi = 0$, $\Delta\varepsilon = 0$, $F = 1$ can be realized. The figure reveals that a shift in valley hopping phase, $\Delta\varphi$, can be compensated by changing ε, which should be experimentally achievable by tuning the applied voltages.

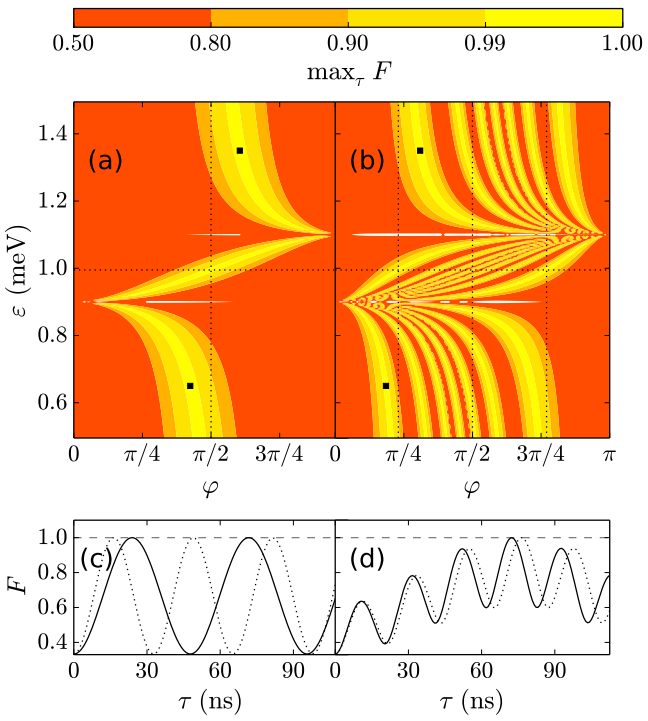

FIG. 3. Gate fidelity F for broad range of the detuning ε and the phase φ in the hopping matrix elements, using same parameters U, h, and t as in Fig. 2. (a,b) F maximized over the gate time τ. We consider the first (a) and fourth (b) local maximum of the fidelity F as a function of time τ. The black squares indicate the positions in parameter space for the time-dependent plots in (c) and (d), namely $\varepsilon = 1.35$ meV for the solid lines and $\varepsilon = 0.65$ meV for the dotted lines in both, (c) and (d), $\varphi = 1.9$ (solid line), $\varphi = 1.333$ (dotted line) in (c), and $\varphi = 0.972$ (solid line), $\varphi = 0.581$ (dotted line) in (d). The horizontal dotted lines in (a) and (b) represent $\varepsilon = \sqrt{U^2 - h^2}$, and the vertical dotted lines belong to values of φ being $\frac{\pi}{2}$ in (a,b) and $\arccos \frac{3}{4}$, $\pi - \arccos \frac{3}{4}$ in (b). Note that the Schrieffer-Wolff transformation breaks down close to $\varepsilon = U \pm h$.

interaction but dominates over exchange in between to realize the valley gate σ_z. In this situation we find $\sigma_z |k\rangle = |k^\perp\rangle$ allowing for the spin SWAP to act for any valley state.

In the case where $\tilde{h}\sigma_z$ is the dominant contribution in $H_{\rm eff}$, we find parameters which allow for a spin SWAP gate, as Fig. 2 and Fig. 3 illustrate. We denote the time evolution according to a time-independent $H_{\rm eff}$ at time τ with $U_{\rm eff}(\tau)$ and consider the average gate fidelity [67]

$$F = \max_{\alpha} \frac{8 + |\,\mathrm{Tr}(e^{i\alpha\sigma_z} U_{\rm eff}(\tau)\mathrm{SWAP}^\dagger)|^2}{72} \qquad (3)$$

where we maximize over a z rotation in valley space which is unimportant for the logical valley qubit in the singlet-triplet subspace. For the spin SWAP gate applied between the dots I and II and between the dots III and IV, the valley z rotation can be different. This difference is equivalent to rotation of the S-T_0 valley qubit, which can be corrected afterwards. In the case $|A|, |B|, |C| \ll |\tilde{h}|$ considered here, we determine the phase α for the maximum in Eq. (3) analytically [66]. Fig. 2 shows F for a detuning around $\varepsilon = \sqrt{U^2 - h^2}$, where the parameter B in Eq. (1) is zero. If furthermore C is negligible, we obtain $U_{\rm eff}(\tau_n) = \mathrm{SWAP}$ for $\varphi = \arccos \frac{n}{n+1}$ and $\tau_n = (n+1)\pi\hbar/A$. In Fig. 2 the situation is shown for $n = 0$ and $n = 3$. Fig. 3 reveals that also for other parameter regimes, $U_{\rm eff}(\tau)$ can be the spin SWAP gate with a high fidelity. The time τ where the maximal fidelity is reached is determined numerically.

Hybrid quantum register.—Now we consider the entire register of n DQDs built in two different ways, as seen in Fig. 1, and prove that universal quantum computing

is possible in these two registers with the interactions assumed in this Letter. For this, it is sufficient to show that single-qubit gates for every qubit and a universal two-qubit gate between arbitrary qubits can be performed [68].

In the register Fig. 1 (a), there is only one spin-only DQD, at position 1, and $(n-1)$ DQDs with spin and valley degree of freedom. Single-qubit gates for the qubits in the k-th DQD, $1 < k \leq n$ can be performed by first transferring these qubits, both spin and valley, to DQD 2. This is done by applying $\mathrm{SWAP}_{\mathrm{spin}} \otimes \mathrm{SWAP}_{\mathrm{valley}}$ gates in the upper and the lower row of the register which allows interchanging the information of DQD k with $k-1$ and so on. The $\mathrm{SWAP}_{\mathrm{spin}} \otimes \mathrm{SWAP}_{\mathrm{valley}}$ gate is provided directly from the exchange interaction [14]. Second, the spin-only SWAP gate transfers the spin qubit into DQD 1 and in return the polarized ancilla spins into DQD 2. Now single-qubit operations can be performed for the spin S-T_0 qubit in DQD 1 and for the valley in DQD 2. The universal two-qubit gate between qubits in DQD k and in DQD m require transferring the qubits from these dots to the DQDs 2 and 3. Then applying the spin-only SWAP moves the spin qubit from DQD 2 to DQD 1. The $\mathrm{SWAP}_{\mathrm{spin}} \otimes \mathrm{SWAP}_{\mathrm{valley}}$ gate between DQDs 2 and 3 and another spin-only SWAP yield a situation where the spin qubit from double dot k and the valley qubit from DQD m are now together in DQD 2 where the universal two-qubit gate can be applied [14]. If two valley qubits or two spin qubits need to be involved in the two-qubit gate, the spin and the valley qubits can be interchanged when they are in DQD 2 as universal gates have been shown to be possible in the building block consisting of DQDs 1 and 2 in this Letter. The average number of additional SWAP gates needed for transferring qubits to the DQD at one end of the register before the desired gates can be applied is in the order of n^2 [66]. The register Fig. 1 (b) contains a spin-only DQD for every spin-valley DQD. This allows for single qubit operations without transferring qubits through the whole register. Two-qubit gates between arbitrary qubits can be performed as spins can be moved within the entire register by spin-only SWAP gates and valley and spin qubits can be interchanged within one building block if necessary. A crucial issue is to achieve high-fidelity SWAP gates, for the spin-only SWAP as well as for the spin and valley SWAP when they are used. Errors in those operations can lead to leakage as spin and valley could leave the singlet-triplet subspaces.

Materials.—We now focus on the materials which may provide the necessary properties for realizing our quantum computation scheme. A natural choice seems to be a hybrid structure of one material without and one with a valley degree of freedom. The crucial point in this situation would be the controlling of the hopping, i.e. parameters t and φ through the interface.

The six-fold valley degeneracy of bulk silicon can be split off by an interface (e.g. between Si and SiO_2) with orientation (001) due to a difference in the effective mass [69, 70] and in Si/SiGe structures also due to strain [71–76]. The positions of the two lower valleys, denoted $|z\rangle$ and $|\overline{z}\rangle$, are in k space on an axis perpendicular to the surface. The other valley states can be neglected. Because of valley-orbit interaction, $|z\rangle$ and $|\overline{z}\rangle$ are coupled, described by the complex matrix element V_{VO} [26]. In experiment, a valley splitting $2|V_{\mathrm{VO}}|$ in lateral silicon quantum dots on the order of 0.1 to 1 meV has been reported [39–46]. In Ref. [45], electrical tunability in the range from 0.3 to 0.8 meV was demonstrated. Calculations show that the phase of the valley-orbit coupling depends on the conduction band offset [29], thus it is different e.g. for Si/SiO_2 or Si/SiGe structures. The phase further depends slightly on the applied electric field [61]. Our scheme demands a non-zero phase difference φ, which is the difference between the phases of V_{VO} in dots I and II or in dots III and IV respectively whereas the phase should be the same for dots II and IV. Furthermore, we need a large valley splitting in dots I and III, which results in a situation where effectively only one valley state has to be considered.

Graphene provides a two-fold valley degeneracy and should in principle allow for a two dimensional array of quantum dots, which is, e.g., not convenient in carbon nanotubes. Theory shows that the valley state is affected by a magnetic field perpendicular to the graphene plane [77] and in graphene nanoribbons also by the boundary conditions [54].

Dual hybrid register.—The roles of spin and valley in the scheme can be exchanged, such that the building block consists of two DQDs, one with spin and valley degree of freedom and the other with valley degree of freedom only. A strong local magnetic field could yield conditions where only the lowest spin states in this DQD have to be taken into account; the spin Zeeman splitting has to be large compared to the exchange interaction, which was e.g. in the order of 0.01 meV in Ref. [3]. To achieve a different phase between this spin states and the spins of the energy eigenstates in the double (spin and valley) degenerated dots, the directions of the magnetic field have to be different at the different dots. Therefore, this alternative approach seems to have less stringent requirements from the material point of view (phase of valley states can be the same), but would require a large gradient of the magnetic field with changes of several Tesla on a nanometer scale.

Conclusion.—In conclusion, we have shown that combining spin and valley singlet-triplet qubits allows for a new hybrid spin-valley quantum computing scheme. Necessary conditions are control over the Zeeman splitting for spin and valley as well as over the phase of the valley states, the realization of high-fidelity SWAP operations, and long enough valley coherence times. The concept relies crucially on the controlled coexistence of spin and valley qubits allowing for universal quantum computing based on the electrically tunable exchange interaction.

Acknowledgements.—We thank the DFG for financial support under the programs SPP 1285 and SFB 767.

[1] D. Loss and D. P. DiVincenzo, Phys. Rev. A **57**, 120 (1998).

[2] For a recent review including both approaches see C. Kloeffel and D. Loss, Annual Review of Condensed Matter Physics **4**, 51 (2013).

[3] J. R. Petta, A. C. Johnson, J. M. Taylor, E. A. Laird, A. Yacoby, M. D. Lukin, C. M. Marcus, M. P. Hanson, and A. C. Gossard, Science **309**, 2180 (2005).

[4] S. Foletti, H. Bluhm, D. Mahalu, V. Umansky, and A. Yacoby, Nature Physics **5**, 903 (2009).

[5] J. Levy, Phys. Rev. Lett. **89**, 147902 (2002).

[6] S. C. Benjamin, Phys. Rev. A **64**, 054303 (2001).

[7] J. Klinovaja, D. Stepanenko, B. I. Halperin, and D. Loss, Phys. Rev. B **86**, 085423 (2012).

[8] R. Li, X. Hu, and J. Q. You, Phys. Rev. B **86**, 205306 (2012).

[9] J. M. Taylor, H.-A. Engel, W. Dur, A. Yacoby, C. M. Marcus, P. Zoller, and M. D. Lukin, Nature Phys. **1**, 177 (2005).

[10] D. Stepanenko and G. Burkard, Phys. Rev. B **75**, 085324 (2007).

[11] G. Ramon, Phys. Rev. B **84**, 155329 (2011).

[12] I. van Weperen, B. D. Armstrong, E. A. Laird, J. Medford, C. M. Marcus, M. P. Hanson, and A. C. Gossard, Phys. Rev. Lett. **107**, 030506 (2011).

[13] M. D. Shulman, O. E. Dial, S. P. Harvey, H. Bluhm, V. Umansky, and A. Yacoby, Science **336**, 202 (2012).

[14] N. Rohling and G. Burkard, New Journal of Physics **14**, 083008 (2012).

[15] For a recent review see F. A. Zwanenburg, A. S. Dzurak, A. Morello, M. Y. Simmons, L. C. L. Hollenberg, G. Klimeck, S. Rogge, S. N. Coppersmith, and M. A. Eriksson, Rev. Mod. Phys. **85**, 961 (2013).

[16] A. H. Castro Neto, F. Guinea, N. M. R. Peres, K. S. Novoselov, and A. K. Geim, Rev. Mod. Phys. **81**, 109 (2009).

[17] F. Kuemmeth, S. Ilani, D. C. Ralph, and P. L. McEuen, Nature **452**, 449 (2008).

[18] M. Shayegan, E. P. De Poortere, O. Gunawan, Y. P. Shkolnikov, E. Tutuc, and K. Vakili, physica status solidi (b) **243**, 3629 (2006).

[19] D. Xiao, G.-B. Liu, W. Feng, X. Xu, and W. Yao, Phys. Rev. Lett. **108**, 196802 (2012).

[20] A. Kormányos, V. Zólyomi, N. D. Drummond, and G. Burkard, Phys. Rev. X **4**, 011034 (2014).

[21] G. Feher and E. A. Gere, Phys. Rev. **114**, 1245 (1959).

[22] A. M. Tyryshkin, S. Tojo, J. J. L. Morton, H. Riemann, N. V. Abrosimov, P. Becker, H.-J. Pohl, T. Schenkel, M. L. W. Thewalt, K. M. Itoh, and S. A. Lyon, Nature Materials **11**, 143 (2012).

[23] T. B. Boykin, G. Klimeck, M. A. Eriksson, M. Friesen, S. N. Coppersmith, P. von Allmen, F. Oyafuso, and S. Lee, Applied Physics Letters **84**, 115 (2004).

[24] M. O. Nestoklon, L. E. Golub, and E. L. Ivchenko, Phys. Rev. B **73**, 235334 (2006).

[25] S. Chutia, S. N. Coppersmith, and M. Friesen, Phys. Rev. B **77**, 193311 (2008).

[26] A. L. Saraiva, M. J. Calderón, X. Hu, S. Das Sarma, and B. Koiller, Phys. Rev. B **80**, 081305 (2009).

[27] D. Culcer, L. Cywiński, Q. Li, X. Hu, and S. Das Sarma, Phys. Rev. B **82**, 155312 (2010).

[28] A. L. Saraiva, B. Koiller, and M. Friesen, Phys. Rev. B **82**, 245314 (2010).

[29] A. L. Saraiva, M. J. Calderón, R. B. Capaz, X. Hu, S. Das Sarma, and B. Koiller, Phys. Rev. B **84**, 155320 (2011).

[30] A. Baena, A. L. Saraiva, B. Koiller, and M. J. Calderón, Phys. Rev. B **86**, 035317 (2012).

[31] D. W. Drumm, A. Budi, M. C. Per, S. P. Russo, and L. C. L. Hollenberg, Nanoscale Research Letters **8**, 1 (2013).

[32] M. De Michielis, E. Prati, M. Fanciulli, G. Fiori, and G. Iannaccone, Applied Physics Express **5**, 124001 (2012).

[33] J. K. Gamble, M. Friesen, S. N. Coppersmith, and X. Hu, Phys. Rev. B **86**, 035302 (2012).

[34] J. K. Gamble, M. A. Eriksson, S. N. Coppersmith, and M. Friesen, Phys. Rev. B **88**, 035310 (2013).

[35] C. Tahan and R. Joynt, Phys. Rev. B **89**, 075302 (2014).

[36] L. Jiang, C. H. Yang, Z. Pan, A. Rossi, A. S. Dzurak, and D. Culcer, Phys. Rev. B **88**, 085311 (2013).

[37] L. Zhang, J.-W. Luo, A. Saraiva, B. Koiller, and A. Zunger, Nature Commun. **4**, 2396 (2013).

[38] A. Dusko, A. L. Saraiva, and B. Koiller, preprint (2013), arXiv:1310.6878.

[39] M. Xiao, M. G. House, and H. W. Jiang, Applied Physics Letters **97**, 032103 (2010).

[40] M. G. Borselli, R. S. Ross, A. A. Kiselev, E. T. Croke, K. S. Holabird, P. W. Deelman, L. D. Warren, I. Alvarado-Rodriguez, I. Milosavljevic, F. C. Ku, W. S. Wong, A. E. Schmitz, M. Sokolich, M. F. Gyure, and A. T. Hunter, Applied Physics Letters **98**, 123118 (2011).

[41] M. G. Borselli, K. Eng, E. T. Croke, B. M. Maune, B. Huang, R. S. Ross, A. A. Kiselev, P. W. Deelman, I. Alvarado-Rodriguez, A. E. Schmitz, M. Sokolich, K. S. Holabird, T. M. Hazard, M. F. Gyure, and A. T. Hunter, Applied Physics Letters **99**, 063109 (2011).

[42] W. H. Lim, C. H. Yang, F. A. Zwanenburg, and A. S. Dzurak, Nanotechnology **22**, 335704 (2011).

[43] C. B. Simmons, J. R. Prance, B. J. Van Bael, T. S. Koh, Z. Shi, D. E. Savage, M. G. Lagally, R. Joynt, M. Friesen, S. N. Coppersmith, and M. A. Eriksson, Phys. Rev. Lett. **106**, 156804 (2011).

[44] C. H. Yang, W. H. Lim, N. S. Lai, A. Rossi, A. Morello, and A. S. Dzurak, Phys. Rev. B **86**, 115319 (2012).

[45] C. H. Yang, A. Rossi, R. Ruskov, N. S. Lai, F. A. Mohiyaddin, S. Lee, C. Tahan, G. Klimeck, A. Morello, and A. S. Dzurak, Nature Commun. **4**, 2069 (2013).

[46] K. Wang, C. Payette, Y. Dovzhenko, P. W. Deelman, and J. R. Petta, Phys. Rev. Lett. **111**, 046801 (2013).

[47] T. M. Kott, B. Hu, S. H. Brown, and B. E. Kane, Phys. Rev. B **89**, 041107 (2014).

[48] B. Roche, E. Dupont-Ferrier, B. Voisin, M. Cobian, X. Jehl, R. Wacquez, M. Vinet, Y.-M. Niquet, and M. Sanquer, Phys. Rev. Lett. **108**, 206812 (2012).

[49] M. Yuan, Z. Yang, C. Tang, A. J. Rimberg, R. Joynt, D. E. Savage, M. G. Lagally, and M. A. Eriksson, (2012), arXiv:1212.0918.

[50] G. Yamahata, T. Kodera, H. O. H. Churchill, K. Uchida, C. M. Marcus, and S. Oda, Phys. Rev. B **86**, 115322 (2012).

[51] X. Hao, R. Ruskov, M. Xiao, C. Tahan, and H. Jiang, preprint (2013), arXiv:1311.5937.

[52] S. Goswami, K. A. Slinker, M. Friesen, L. M. McGuire, J. L. Truitt, C. Tahan, L. J. Klein, J. O. Chu, P. M. Mooney, D. W. van der Weide, R. Joynt, S. N. Coppersmith, and M. A. Eriksson, Nature Phys. **3**, 41 (2007).

[53] M. A. Eriksson, M. Friesen, S. N. Coppersmith, R. Joynt, L. J. Klein, K. Slinker, C. Tahan, P. M. Mooney, J. O. Chu, and S. J. Koester, Quantum Information Processing **3**, 133 (2004).

[54] B. Trauzettel, D. V. Bulaev, D. Loss, and G. Burkard, Nature Phys. **3**, 192 (2007).

[55] B. M. Maune, M. G. Borselli, B. Huang, T. D. Ladd, P. W. Deelman, K. S. Holabird, A. A. Kiselev, I. Alvarado-Rodriguez, R. S. Ross, A. E. Schmitz, M. Sokolich, C. A. Watson, M. F. Gyure, and A. T. Hunter, Nature **481**, 344 (2012).

[56] A. Pályi and G. Burkard, Phys. Rev. Lett. **106**, 086801 (2011).

[57] G. Y. Wu, N.-Y. Lue, and L. Chang, Phys. Rev. B **84**, 195463 (2011).

[58] G. Y. Wu, N.-Y. Lue, and Y.-C. Chen, Phys. Rev. B **88**, 125422 (2013).

[59] D. Culcer, X. Hu, and S. Das Sarma, Phys. Rev. B **82**, 205315 (2010).

[60] D. Culcer, A. L. Saraiva, B. Koiller, X. Hu, and S. Das Sarma, Phys. Rev. Lett. **108**, 126804 (2012).

[61] Y. Wu and D. Culcer, Phys. Rev. B **86**, 035321 (2012).

[62] K. I. Kugel and D. I. Khomskii, Zh. Eksp. Teor. Fiz **64**, 1429 (1973).

[63] B. E. Kane, Nature **393**, 133 (1998).

[64] L. M. K. Vandersypen, R. Hanson, L. H. W. van Beveren, J. M. Elzerman, J. S. Greidanus, S. D. Franceschi, and L. P. Kouwenhoven, in *Quantum Computing and Quantum Bits in Mesoscopic Systems* (Kluwer Academic/Plenum, New York, 2003) arXiv:quant-ph/0207059.

[65] G. Burkard and A. Imamoglu, Phys. Rev. B **74**, 041307 (2006).

[66] See Supplemental Material.

[67] L. H. Pedersen, N. M. Møller, and K. Mølmer, Physics Letters A **367**, 47 (2007).

[68] D. P. DiVincenzo, Phys. Rev. A **51**, 1015 (1995).

[69] T. Ando, A. B. Fowler, and F. Stern, Rev. Mod. Phys. **54**, 437 (1982).

[70] B. E. Kane, N. S. McAlpine, A. S. Dzurak, R. G. Clark, G. J. Milburn, H. B. Sun, and H. Wiseman, Phys. Rev. B **61**, 2961 (2000).

[71] C. Herring, Bell System Technical Journal **34**, 237 (1955).

[72] C. Herring and E. Vogt, Phys. Rev. **101**, 944 (1956).

[73] C. G. Van de Walle and R. M. Martin, Phys. Rev. B **34**, 5621 (1986).

[74] R. People and J. C. Bean, Appl. Phys. Lett. **48**, 538 (1986).

[75] M. M. Rieger and P. Vogl, Phys. Rev. B **48**, 14276 (1993).

[76] F. Schäffler, Semiconductor Science and Technology **12**, 1515 (1997).

[77] P. Recher, J. Nilsson, G. Burkard, and B. Trauzettel, Phys. Rev. B **79**, 085407 (2009).

Supplemental Material

A. SCHRIEFFER-WOLFF TRANSFORMATION

The Schrieffer-Wolff transformation for our Hamiltonian from the main text,

$$\tilde{H} = e^{-S} H e^{S} \approx H_0 + H_V + \frac{[H_T, S]}{2} = \begin{pmatrix} H_{\text{eff}} & 0 \\ 0 & H_{\text{as}} \end{pmatrix}, \tag{A1}$$

is done similar to the situation without the valley degree of freedom [S1]. The block H_{eff} describes the physics in the low-energy subspace, which has approximately (1,1) charge configuration when the detuning ε is close to zero. We can perform the transformation for the spin singlet subspace and for the spin triplet subspaces separately. The projection on the three-dimensional subspace including one spin triplet, is spanned e.g. by the basis $\{|\uparrow,\uparrow+\rangle = \hat{c}^{\dagger}_{1\uparrow}\hat{c}^{\dagger}_{2\uparrow+}|0\rangle, |\uparrow,\uparrow-\rangle\, \hat{c}^{\dagger}_{1\uparrow}\hat{c}^{\dagger}_{2\uparrow-}|0\rangle, |0,\uparrow+\uparrow-\rangle = \hat{c}_{2\uparrow+}\hat{c}_{2\uparrow-}|0\rangle\}$ for the T_+ triplet and described by the Hamiltonian,

$$H_{\text{Triplet}} = \begin{pmatrix} h & 0 & -t_- \\ 0 & -h & t_+ \\ -t_-^* & t_+^* & U-\varepsilon \end{pmatrix}. \tag{A2}$$

For the spin singlet subspace we have in the basis $\{(|\uparrow,\downarrow+\rangle - |\downarrow,\uparrow+\rangle)/\sqrt{2}, (|\uparrow,\downarrow-\rangle - |\downarrow,\uparrow-\rangle)/\sqrt{2}, (|0,\uparrow+\downarrow-\rangle + |0,\uparrow-\downarrow+\rangle)/\sqrt{2}, |(\uparrow\downarrow,0)\rangle, |0,\uparrow+\downarrow+\rangle, |0,\uparrow-\downarrow-\rangle\}$, the Hamiltonian

$$H_{\text{Singlet}} = \begin{pmatrix} h & 0 & t_- & \sqrt{2}t_+^* & \sqrt{2}t_+ & 0 \\ 0 & h & t_+ & \sqrt{2}t_-^* & 0 & \sqrt{2}t_-^* \\ t_-^* & t_+^* & U-\varepsilon & 0 & 0 & 0 \\ \sqrt{2}t_+ & \sqrt{2}t_- & 0 & U+\varepsilon & 0 & 0 \\ \sqrt{2}t_+^* & 0 & 0 & 0 & U-\varepsilon+2h & 0 \\ 0 & \sqrt{2}t_-^* & 0 & 0 & 0 & U-\varepsilon-2h \end{pmatrix}. \tag{A3}$$

The anti-Hermitian matrix S should obey $[H_0 + H_V, S] = -H_T$, which is fulfilled if the blocks corresponding to the singlet and triplet subspaces are given by

$$S_{\text{Triplet}} = \begin{pmatrix} 0 & 0 & \frac{t_-}{h-U+\varepsilon} \\ 0 & 0 & \frac{-t_+}{-h-U+\varepsilon} \\ \frac{-t_-^*}{h-U+\varepsilon} & \frac{t_+^*}{-h-U+\varepsilon} & 0 \end{pmatrix} \tag{A4}$$

and

$$S_{\text{Singlet}} = \begin{pmatrix} 0 & 0 & \frac{-t_-}{h-U+\varepsilon} & \frac{\sqrt{2}t_+^*}{-h+U+\varepsilon} & \frac{-\sqrt{2}t_+}{-h-U+\varepsilon} & 0 \\ 0 & 0 & \frac{-t_+}{-h-U+\varepsilon} & \frac{\sqrt{2}t_-^*}{h+U+\varepsilon} & 0 & \frac{-\sqrt{2}t_-}{h-U+\varepsilon} \\ \frac{t_-^*}{h-U+\varepsilon} & \frac{t_+^*}{-h-U+\varepsilon} & 0 & 0 & 0 & 0 \\ \frac{-\sqrt{2}t_+}{-h+U+\varepsilon} & \frac{-\sqrt{2}t_-}{h+U+\varepsilon} & 0 & 0 & 0 & 0 \\ \frac{\sqrt{2}t_+^*}{-h-U+\varepsilon} & 0 & 0 & 0 & 0 & 0 \\ 0 & \frac{\sqrt{2}t_-^*}{h-U+\varepsilon} & 0 & 0 & 0 & 0 \end{pmatrix}. \tag{A5}$$

This leads to the effective Hamiltonian given in Eq. (1) of the main text.

B. TIME EVOLUTION WITH THE EFFECTIVE HAMILTONIAN

The time evolution according to the effective Hamiltonian,

$$H_{\text{eff}} = [(A\cos\varphi + B)\mathbb{1} + (A + B\cos\varphi)\sigma_z + B\sin\varphi\,\sigma_y]\, P_S + \tilde{h}\sigma_z + C\,[(1-\cos\varphi)\mathbb{1} - \sin\varphi\,\sigma_y], \tag{B1}$$

can be considered separately for the spin singlet subspace and for the three spin triplet subspaces, where the latter are identical to each other. We denote the two-dimensional effective Hamiltonians for the singlet and one of the triplet subspaces by

$$H_{\rm eff}^S = (A\cos\varphi{+}B{+}C(1-\cos\varphi))\mathbb{1} + (\tilde{h}{+}A{+}B\cos\varphi)\sigma_z + (B-C)\sin\varphi\,\sigma_y \tag{B2}$$

and

$$H_{\rm eff}^T = \tilde{h}\sigma_z + C\left[(1-\cos\varphi)\mathbb{1} - \sin\varphi\,\sigma_y\right]. \tag{B3}$$

By introducing

$$\theta_S = \sqrt{(\tilde{h}{+}A{+}B\cos\varphi)^2 + (B-C)^2\sin^2\varphi}, \qquad \mathbf{n}_S = \frac{(B-C)\sin\varphi}{\theta_S}\mathbf{e}_y + \frac{\tilde{h}{+}A{+}B\cos\varphi}{\theta_S}\mathbf{e}_z, \tag{B4}$$

$$\theta_T = \sqrt{\tilde{h}^2 + C^2\sin^2\varphi}, \qquad \mathbf{n}_T = \frac{-C\sin\varphi}{\theta_T}\mathbf{e}_y + \frac{\tilde{h}}{\theta_T}\mathbf{e}_z, \tag{B5}$$

we find for the corresponding time evolution operators

$$U_S(\tau) = e^{-iH_{\rm eff}^S\tau/\hbar} = e^{-i(A\cos\varphi{+}B{+}C(1-\cos\varphi))\tau/\hbar}(\cos(\theta_S\tau/\hbar)\mathbb{1} - i\sin(\theta_S\tau/\hbar)\mathbf{n}_S\cdot\boldsymbol{\sigma}), \tag{B6}$$

$$U_T(\tau) = e^{-iH_{\rm eff}^T\tau/\hbar} = e^{-iC(1-\cos\varphi)\tau/\hbar}(\cos(\theta_T\tau/\hbar)\mathbb{1} - i\sin(\theta_T\tau/\hbar)\mathbf{n}_T\cdot\boldsymbol{\sigma}). \tag{B7}$$

In a basis with spin singlet and triplet states, say $\{|T_+{+}\rangle, |T_+{-}\rangle, |T_0{+}\rangle, |T_0{-}\rangle, |T_-{+}\rangle, |T_-{-}\rangle, |S{+}\rangle, |S{-}\rangle\}$ where $\pm$ denotes the valley state of the electron in the right dot and T_+, T_-, T_0, S the spin state, e.g., $|T_+{+}\rangle = |\uparrow,\uparrow{+}\rangle$, the time evolution operator $U_{\rm eff}$ is block diagonal,

$$U_{\rm eff}(\tau) = \begin{pmatrix} U_T(\tau) & 0 & 0 & 0 \\ 0 & U_T(\tau) & 0 & 0 \\ 0 & 0 & U_T(\tau) & 0 \\ 0 & 0 & 0 & U_S(\tau) \end{pmatrix}. \tag{B8}$$

The average fidelity of this operation with respect to a spin SWAP gate, $\mathrm{SWAP} = \mathrm{SWAP}^\dagger = \mathrm{diag}(1,1,1,1,1,1,-1,-1)$ in our basis, maximized over a unimportant z rotation in valley space is given by (see [S2] for general formula)

$$F = \max_\alpha \frac{8 + |\operatorname{Tr}(e^{i\alpha\sigma_z}U_{\rm eff}(\tau)\mathrm{SWAP})|^2}{8(8+1)} = \max_\alpha \frac{8 + |3\operatorname{Tr}(e^{i\alpha\sigma_z}U_T(\tau)) - \operatorname{Tr}(e^{i\alpha\sigma_z}U_S(\tau))|^2}{72} \tag{B9}$$

and $T(\tau) := \frac{1}{4}|3\operatorname{Tr}(e^{i\alpha\sigma_z}U_T(\tau)) - \operatorname{Tr}(e^{i\alpha\sigma_z}U_S(\tau))|^2$ is according to (B6) and (B7) given by

$$T(\tau) = |3(\cos\alpha\cos(\theta_T\tau/\hbar) - \sin\alpha\sin(\theta_T\tau/\hbar)n_{Tz}) - e^{i(A\cos\varphi+B)\tau/\hbar}(\cos\alpha\cos(\theta_S\tau/\hbar) - \sin\alpha\sin(\theta_S\tau/\hbar)n_{Sz})|^2. \tag{B10}$$

For $|A|, |B|, |C| \ll |\tilde{h}|$ we find the first order approximations

$$\theta_T \approx \tilde{h}, \qquad \theta_S \approx \tilde{h} + A + B\cos\varphi, \qquad \text{and} \qquad n_{Tz} \approx n_{Sz} \approx 1 \tag{B11}$$

leading to

$$\begin{aligned} T(\tau) =& [3\cos(\alpha{+}\tilde{h}\tfrac{\tau}{\hbar}) - \cos((A\cos\varphi{+}B)\tfrac{\tau}{\hbar})\cos(\alpha{+}(\tilde{h}{+}A{+}B\cos\varphi)\tfrac{\tau}{\hbar})]^2 \\ &+ \sin^2((A\cos\varphi{+}B)\tfrac{\tau}{\hbar})\cos^2(\alpha{+}(\tilde{h}{+}A{+}B\cos\varphi)\tfrac{\tau}{\hbar}) \\ =& 9\cos^2(\alpha{+}\tilde{h}\tfrac{\tau}{\hbar}) + \cos^2(\alpha{+}(\tilde{h}{+}A{+}B\cos\varphi)\tfrac{\tau}{\hbar}) - 6\cos(\alpha{+}\tilde{h}\tfrac{\tau}{\hbar})\cos(\alpha{+}(\tilde{h}{+}A{+}B\cos\varphi)\tfrac{\tau}{\hbar})\cos((A\cos\varphi{+}B)\tfrac{\tau}{\hbar})]. \end{aligned} \tag{B12}$$

To find the value of α which gives the maximal average fidelity F, we calculate

$$0 \stackrel{!}{=} \frac{\partial T(\tau)}{\partial\alpha} = -9\sin(2\alpha{+}2\tilde{h}\tfrac{\tau}{\hbar}) - \sin(2\alpha{+}2(\tilde{h}{+}A{+}B\cos\varphi)\tfrac{\tau}{\hbar}) + 6\cos((A\cos\varphi{+}B)\tfrac{\tau}{\hbar})\sin(2\alpha{+}(2\tilde{h}{+}A{+}B\cos\varphi)\tfrac{\tau}{\hbar}), \tag{B13}$$

which is solved by

$$\alpha = -\tilde{h}\frac{\tau}{\hbar} + \frac{1}{2}\arctan\frac{6\cos((A\cos\varphi+B)\frac{\tau}{\hbar})\sin((A+B\cos\varphi)\frac{\tau}{\hbar}) - \sin(2(A+B\cos\varphi)\frac{\tau}{\hbar})}{9 + \cos(2(A+B\cos\varphi)\frac{\tau}{\hbar}) - 6\cos((A\cos\varphi+B)\frac{\tau}{\hbar})\cos((A+B\cos\varphi)\frac{\tau}{\hbar})}, \tag{B14}$$

where the dominant term is $-\tilde{h}\frac{\tau}{\hbar}$. The maximization with respect to τ is done numerically by using minimization of $1-F$, for the Figures 2 and 3 of the main text we calculate F according to Eq. (B9) with the (approximate) maximization value for α from (B14).

C. FIDELITY AROUND FIRST, SECOND, THIRD, AND FOURTH LOCAL MAXIMUM

In order to find more phases in the hopping matrix element, φ, where the spin-only SWAP gate can be realized, we calculate F for a broader range of ε and φ than it was done for Fig. 2. We consider the first, second, third, and fourth local maximum of the fidelity as a function of time, $F(\tau)$. The results are shown in Fig. C1.

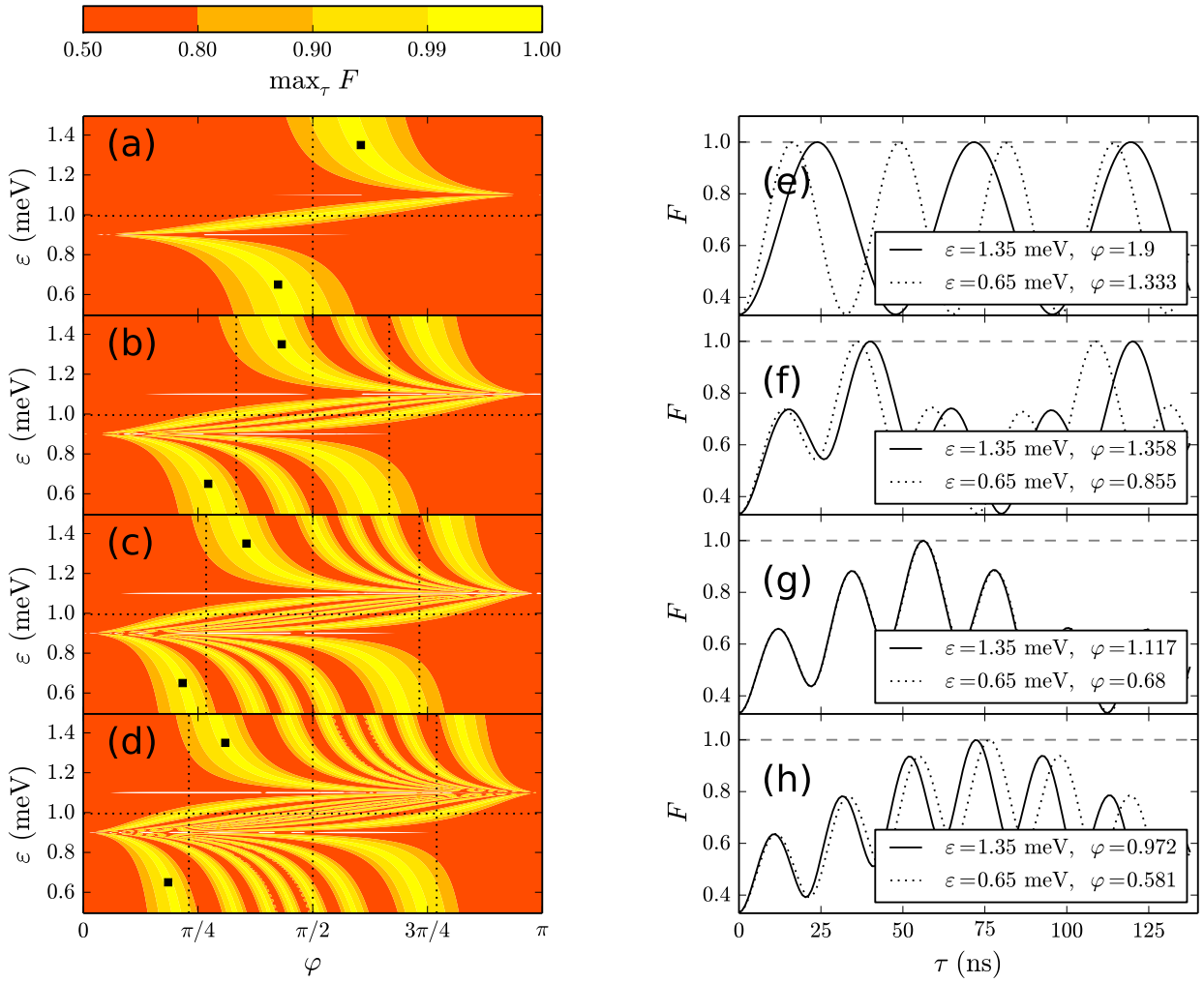

Fig. C1. Fidelity F for a broader range of the detuning ε and the phase in the hopping matrix elements, φ; the parameters U, h, and t are the same as in Fig. 2. (a-d) F maximized over the gate time τ (scale bar). We consider the first (a), second (b), third (c), and fourth (d) local maximum of F. The black squares indicates the parameters for the time-dependent plots in (e)-(h). The horizontal dotted lines in (a-d) represent $\varepsilon = \sqrt{U^2-h^2}$, and the vertical dotted lines belong to values of φ being $\frac{\pi}{2}$ (a-d); $\frac{\pi}{3}$, $\frac{2\pi}{3}$ (b); $\arccos\frac{2}{3}$, $\pi-\arccos\frac{2}{3}$ (c); $\arccos\frac{3}{4}$, $\pi-\arccos\frac{3}{4}$ (d). Note that the Schrieffer-Wolff transformation breaks down close to $\varepsilon = U \pm h$.

D. EXPLICIT SEQUENCES FOR QUANTUM GATES

In this section we give explicit sequences which show how single- and two-qubit gates can be applied in the two registers shown in Fig. 1 of the main text. In following we consider first the register Fig. 1 (a) and after that Fig. 1 (b). We introduce the notation $\mathrm{SWAP}_{sv}(m, m-1)$ for the $\mathrm{SWAP}_{\mathrm{spin}} \otimes \mathrm{SWAP}_{\mathrm{valley}}$ gate applied at the upper and the lower lines of the register between the dots at position m and $m-1$. This gate is provided for dots with spin and valley degeneracy directly by exchange interaction [S3], i.e., in Fig. 1 (a) they can be applied for $m \leq 3$. Furthermore we denote the spin-only SWAP gate between the dots at position m and $m-1$, applied again in the upper and the lower line of the register, by $\mathrm{SWAP}_s(m, m-1)$. This gate can be performed for the register Fig. 1 (a) for $m = 2$ and for Fig. 1 (b) for any $m = 2, 3, 4, \ldots$ The single qubit gates of the valley qubit in the k-th double quantum dot (DQD) in Fig. 1 (a) are realized by the four steps below:

1. Apply $\mathrm{SWAP}_{sv}(k, k-1), \mathrm{SWAP}_{sv}(k-1, k-2), \ldots, \mathrm{SWAP}_{sv}(3, 2)$.
2. Apply $\mathrm{SWAP}_s(2, 1)$.
3. Perform the single-qubit operation in DQD 2.
4. Repeat the second step and then the first in inverse order to bring the qubits back to position k.

The exchange interaction and a gradient in the valley splitting provides full control over two axis in Bloch sphere of the valley qubit and thus allow for the third step. Single-qubit operations with the S-T_0 spin triplet are done the same way using exchange and a gradient in the spin Zeeman field of DQD 1 within step 3 of the given procedure. For a two-qubit gate between the valley qubits of DQD k and m with $m > k$ the steps are as follows:

1. Apply $\mathrm{SWAP}_{sv}(k, k-1), \mathrm{SWAP}_{sv}(k-1, k-2), \ldots, \mathrm{SWAP}_{sv}(3, 2)$ and $\mathrm{SWAP}_{sv}(m, m-1), \mathrm{SWAP}_{sv}(m-1, m-2), \ldots, \mathrm{SWAP}_{sv}(4, 3)$.
2. Apply a SWAP gate between the spin and the valley qubit residing in DQD k. This is possible as any unitary operation is feasible in this subsystem.
3. Apply $\mathrm{SWAP}_s(2, 1)$.
4. Apply $\mathrm{SWAP}_{sv}(3, 2)$.
5. Apply $\mathrm{SWAP}_s(2, 1)$.
6. Apply the two-qubit gate between the spin and the valley qubit in DQD 2, which are the former valley qubits of DQDs k and m.
7. Return the qubits to their former position by reversing steps 1 to 5.

For a two-qubit gate between a spin and a valley qubit, step 2 is not necessary and between two spin qubits, step 2 exchanges the spin and valley qubits from the m-th instead of the k-th DQD.

We proved that universal quantum computing is possible in Fig. 1 (a), but should also ask how efficient our scheme is, in particular, whether it scales polynomially or not. To answer this question, we first count the number of gates needed for a single-qubit operation each on the whole $2n-2$ qubits. We remember for a single gate on a qubit in the k-th DQD we need each $2k-2$ $\mathrm{SWAP}_{\mathrm{spin}} \otimes \mathrm{SWAP}_{\mathrm{valley}}$ gates for swapping the qubits to position 2 and back and two spin-only SWAP gates. Then the $(k-1)$-th qubit needs $2k-2$ gates and so on, resulting in a total of $4 \sum_{k=0}^{n} k = O(n^2)$ needed gates.

Now we consider Fig. 1 (b) and prove universality alike the register in Fig. 1 (a). The single-qubit gates are directly given by the alternating structure of the register. For the two-qubit gates between two valley qubits in DQD k and $m > k$ the steps are as follows:

1. Swap the valley qubits with the spin qubit in DQD m.
2. Apply $\mathrm{SWAP}_s(m, m-1), \mathrm{SWAP}_s(m-1, m-2), \ldots, \mathrm{SWAP}_s(k+1, k)$.
3. Apply the two-qubit gate between the spin and the valley in DQD m.
4. Return the qubits to their former position by reversing step 2 and 1.

For a two-qubit gate between a spin and a valley qubit, step 1 is not necessary and between two spin qubits step 2 interchanges the spin and the valley from the m-th instead of the k-th qubit.

[S1] G. Burkard and A. Imamoglu, Phys. Rev. B **74**, 041307 (2006).

[S2] L. H. Pedersen, N. M. Møller, and K. Mølmer, Physics Letters A **367**, 47 (2007).

[S3] N. Rohling and G. Burkard, New Journal of Physics **14**, 083008 (2012).